

Study of the performances of the shield and muon veto of the XENON1T experiment.

Marco SELVI*

(on behalf of the XENON1T collaboration)

INFN - Bologna

E-mail: selvi@bo.infn.it

Within the XENON program, we are operating a double-phase time-projection chamber (TPC) using liquid xenon (LXe) as target material. The current phase, XENON100 installed in the LNGS, is in science mode since the beginning of 2010, with a sensitivity goal of 2×10^{-45} cm² for spin-independent WIMP-nucleon scattering. For the next step, we propose to build a detector with a total mass of 2.4 tons of LXe (1.2 fiducial): XENON1T. The goal is to reduce the background by two orders of magnitude with respect to XENON100, reaching a sensitivity of about 5×10^{-47} cm². Therefore it is crucial to reduce the external backgrounds: gammas and neutrons from the ambient radioactivity and the most dangerous muon-induced neutrons. A study of the shield and muon veto needed by the experiment has been carried on with a full Geant4 Monte Carlo simulation. To shield the experiment at LNGS we plan to build a water tank of 10 m diameter and 10 m height, instrumented with PMTs to act as a Cerenkov muon veto. The results of the simulation show that the gammas and neutrons from rock and concrete radioactivity are reduced at a completely negligible level, and the muon-induced neutrons contribute to mimic the WIMP's signal with 0.07 events per year, which allows to reach the foreseen sensitivity of the experiment.

Identification of Dark Matter 2010

July 26 - 30 2010

University of Montpellier 2, Montpellier, France

*Speaker.

1. Introduction

Within the XENON program, we are operating a detector based on the simultaneous measurement of the ionization and scintillation signals produced by a WIMP interaction in the sensitive volume of a 3D-position sensitive TPC filled with high purity liquid xenon. The current phase, XENON100 installed in the LNGS, is in science mode since the beginning of 2010, with a sensitivity goal of $2 \times 10^{-45} \text{ cm}^2$ for spin-independent WIMP-nucleon scattering cross section.

The analysis of 11.2 live days of background data taken during a commissioning run in fall 2009 leads to the first science result of XENON100: no events are observed in the 40 kg fiducial volume, excluding spin-independent WIMP-nucleon scattering cross sections above $3.4 \times 10^{-44} \text{ cm}^2$ (at $100 \text{ GeV}/c^2$), see [1, 2] for further details.

For the next step, we propose to build a detector with a total mass of 2.4 tons of LXe (1.2 fiducial): XENON1T. The goal is to reduce the background rate at the level of $0.1 \times 10^{-3} \text{ counts/keV/kg/day}$ ($\equiv \text{dru}$), two orders of magnitude lower than XENON100, reaching a sensitivity of about $5 \times 10^{-47} \text{ cm}^2$.

2. The detector design

The detector of XENON1T is a double-phase (liquid/gas) time projection chamber. Any interaction inside the active liquid xenon volume of the TPC generates prompt primary scintillation light (S1) and ionizes the LXe. A strong electric field (the drift field) across the TPC extracts the ionization electrons from the interaction site and drifts them towards the xenon gas phase above the liquid. The electrons are extracted into the gas phase with a second electric field (the extraction field), where they generate a secondary scintillation signal (S2) which is directly proportional to the charge. The event's interaction site can be reconstructed using the very localized S2 signal (xy) and the time difference between the prompt and the secondary scintillation signal (z). Discrimination between nuclear-recoil-like signals and electron-recoil-like background based on their different S2/S1 ratio is possible to $> 99 \%$. Primary and secondary scintillation signal are both detected with two arrays of photo-sensors, one immersed in the LXe below the cylindrical TPC, and a second one located in the xenon gas above the target volume. In order to reach the design sensitivity, all materials close to the target volume have to be of very low intrinsic radioactivity. This requirement is of particular importance for the photo-sensors. The proposed solution is based on 3" diameter QUPIDs [3], a novel hybrid photo-detector with very low radioactivity, however, it can be adapted to any other 3" photo-sensor easily. Each array (top and bottom) is made of 121 QUPIDs.

The TPC is made of PTFE panels forming a cylinder of about 1 m diameter and 1 m height. The cryostat is a double-walled super-insulated pressure vessel. The inner vessel houses the liquid xenon (at a temperature of $\sim 180 \text{ K}$), the TPC as well as the photo-sensors. The outer one is a vacuum vessel to thermally decouple the inner vessel from ambient temperature. The material choice is between stainless steel and titanium; for both options the foreseen thickness is of about 5 mm for each vessel.

There are currently two options for the underground laboratory and the shield:

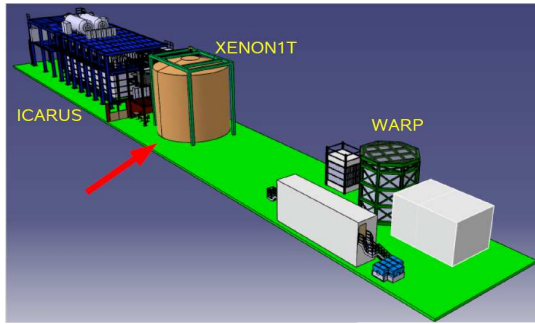


Figure 1: Sketch of the Hall B of LNGS with the proposed location for the XENON1T experiment.

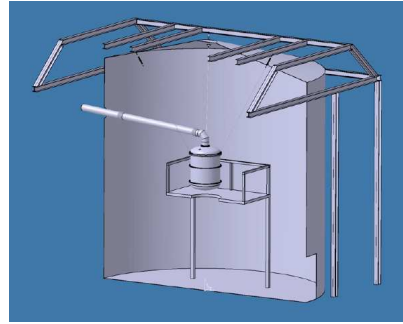


Figure 2: The cryostat hosting the XENON1T detector, placed in the center of the water tank.

- LNGS with the cryostat immersed in a water tank of 10 m diameter and 10 m height, instrumented with PMTs to act as a Cerenkov muon veto;
- LSM (where the muon flux is reduced by about a factor 50 with respect to LNGS, because of its larger rock overburden) with a conventional lead-polyethylene passive shield with a plastic scintillator muon veto all around it.

In this work we describe the performances of the active water shield at the LNGS depth, while the results of the study for the passive shield at LSM are presented in a separate contribution [4]. A sketch of the Hall B at LNGS with the proposed location for the experiment is shown in Fig. 1 and the water tank with the cryostat in Fig. 2.

3. MC simulation

A detailed Monte Carlo simulation has been developed with the GEANT4 code [5] (version 9.3), describing in detail all the components of the detector, cryostat and shield.

Since GEANT4 offers alternative models to treat certain physics processes, we mention here briefly which ones were used in these simulations¹. Muon-induced spallation (or muon photo-nuclear interaction) is modeled above 1 GeV muon energy; the final-state generator relies on parametrized hadronic models. Gamma inelastic scattering, the real photo-nuclear interaction, generates its hadronic final states using a chiral-invariant phase-space decay model below 3 GeV; a theoretical quark-gluon string model simulates the punch-through reaction at higher energies. The hadronic interaction of nucleons, pions and kaons is simulated with the quark-gluon string model above 6 GeV, an intra-nuclear binary cascade model at lower energies and a pre-equilibrium de-excitation stage below 70 MeV. The equilibrium stage considers fragment and gamma evaporation, fission, Fermi break-up and multi-fragmentation of highly-excited nuclei. Neutron transport and interactions are described by data-driven models below 19 MeV. The elastic scattering of hadrons above 20 MeV is described by the *G4LElastic* model. The choice of electromagnetic physics is more straightforward and will not be described here.

¹The physics list here described is derived from the advanced example called “cosmicray_charging”, available in the GEANT4 package up to the version 9.2, with the addition of the high precision (HP) treatment of neutron interaction below 19 MeV. The same physics list was used in other studies about neutron production and propagation, e.g. [6]

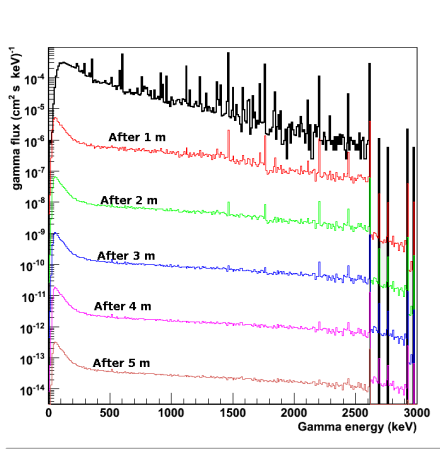


Figure 3: Black: gamma energy spectrum in the LNGS hall B. Colored lines: gamma energy spectrum after each meter of the water shield.

4. External backgrounds

The sources of external backgrounds potentially dangerous for dark matter search in an underground laboratory are mainly:

- gammas from rock and concrete radioactivity,
- low energy neutrons (< 10 MeV) from rock and concrete radioactivity,
- high energy neutrons (up to tens of GeV) produced by muons in the rock or in the detector and shield materials.

Gammas from rock and concrete radioactivity In Fig. 3 the energy spectrum of gamma rays in the Hall B is shown (black line). It was measured with a 2'' NaI detector and the detector acceptance has been determined using a GEANT4 simulation. We also performed a MC simulation with GEANT4 considering various layers of water. In Fig. 3 the colored lines are the energy spectrum of the survived gammas after each meter of water shield. The total flux outside the shield is about $1 \text{ cm}^{-2}\text{s}^{-1}$, in agreement with other measurements done in the LNGS (see e.g. [7]). The gamma reduction after each meter of water is shown in Fig. 4. For comparison, we verified that the flux reduction after 3 m of water is slightly better than after a conventional gamma shield made of 20 cm of lead.

We considered the gamma energy spectrum after 3 m of water (where the flux is reduced by a factor $\sim 10^6$) and we use it as input for a detailed GEANT4 simulation of the XENON1T detector, generating the gammas uniformly and isotropically just outside the cryostat. In Fig. 5 we show the number of single scatter events in the whole LXe (2.4 ton, black line) and in the fiducial volume (FDV), that is removing the outermost 10 cm (1.2 ton, red line). In the fiducial volume the rate of events is very low, in particular in the dark matter search energy window (corresponding to 2–15 keVee) we will have less than 10^{-8} dru (i.e. about 0.05 evts/ton/year) in the 1.2 ton FDV before

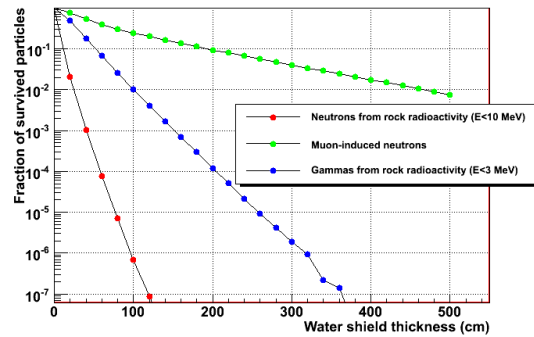


Figure 4: Fraction of surviving particles in the water shield: gamma (blue) and neutrons (red) from rock and concrete radioactivity, muon-induced neutrons (green).

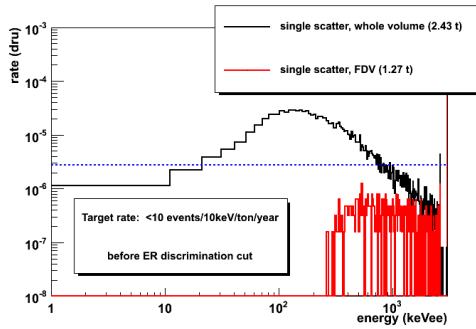


Figure 5: Energy spectrum of the single scatters recoils in the whole 2.4 ton LXe volume (black) and in the 1.2 ton fiducial volume (red) produced by the gammas from rock and concrete radioactivity after the shield made of 3 m of water. Rates are calculated before performing the electron recoil discrimination cut. The blue dashed line shows the foreseen goal for the background of the XENON1T experiment.

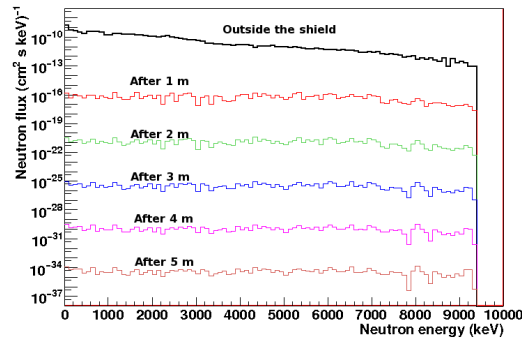


Figure 6: Black: energy spectrum of the neutrons from concrete radioactivity in the LNGS. Colored lines: neutron energy spectrum after each meter of the water shield.

the ER rejection cut, well below the background level tolerated by the experiment (dashed blue line).

Thus, the conclusion is that 3 m of water are enough to shield the external gammas from ambient radioactivity.

Neutrons from rock and concrete radioactivity Neutrons are produced mainly from ^{238}U fission and (α, n) reactions and from ^{232}Th (α, n) reactions in the concrete that surrounds the LNGS halls. The neutron energy spectra have been obtained with the modified SOURCES code, considering the following concentrations: $[\text{U}]=1.05$ ppm, $[\text{Th}]=0.656$ ppm [8]. We generate the neutrons inside a layer of 30 cm of concrete; in Fig. 6 (black) it is shown the energy spectrum of the neutrons as they come out of the concrete. The total flux above 1 keV is $8.7 \times 10^{-7} \text{ (cm}^2 \text{ s)}^{-1}$, in good agreement with the results of the measurements and the simulation listed in [8].

The water shield is very effective in shielding MeV neutrons: with our G4 simulation, as shown in Fig. 6 (red), we obtain, after 1 m, a reduction of more than a factor 10^6 . Thus this source of background is shielded at a completely negligible level by few meters of water.

Muon-induced neutrons in the rock Neutrons are produced via direct muon spallation with the nuclei or through the electromagnetic and hadronic cascades generated by the muon. Though their flux is about 3 orders of magnitude lower than that of neutrons from concrete radioactivity, their energy spectrum extends up to tens of GeV, thus they are very hard to shield. Moreover their lateral displacement can be of several meters, thus even with an active veto all around the detector there is the possibility that the muon is not tagged but its associated neutrons can still penetrate into the shield.

The neutron energy spectrum at the surface between the rock and the LNGS hall is obtained with a complete GEANT4 simulation of the LNGS laboratory with a minimum amount of 5 m of rock around the experimental hall. Cosmic muons are generated with the proper energy and angular

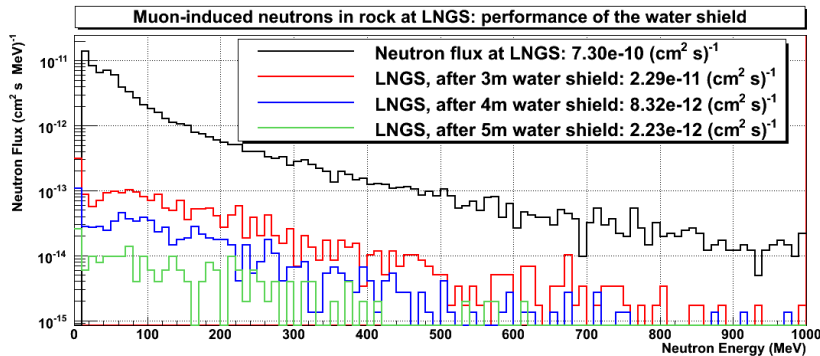


Figure 7: Black: energy spectrum of the neutrons produced by muons in the rock at LNGS. Colored lines: energy spectrum of the neutrons that survive after 3, 4 and 5 m of the water shield.

distribution and all the secondaries are followed and tracked down to the hall. In this way we have the exact correlation between the position of the primary muon and of the induced neutrons. Since it is known that GEANT4 underestimates the neutron production [6], the neutron flux obtained is normalized to the value found in [10] with FLUKA: $7.3 \cdot 10^{-10} \text{ n}/(\text{cm}^2 \text{ s})$ for $E_n > 10 \text{ MeV}$.

Detecting the muons through their Cerenkov light in the water tank allows to tag the associated neutrons. Depending on the water buffer size (3, 4 or 5 m) the percentage of neutrons that are tagged is, respectively, about: 20, 30, 40%, with respect to the flux of neutrons at the surface of the water tank. The most important reduction is given by the water shield itself: 96, 98, 99.5% of the neutrons are moderated and stopped by the 3, 4, 5 m water buffer. The total reduction given by the muon veto and the shield moderation leads to the following fraction of neutrons (with respect to the original ones coming from the rock): 3.1, 1.1, 0.3%; the energy spectra of the survived neutrons are shown in Fig. 7.

In Tab. 1, we summarize the performances of the various sizes of water buffer shield; the fraction of surviving neutrons as a function of the water buffer thickness can be seen also in Fig. 4 (green points).

	3m buffer	%	4m buffer	%	5m buffer	%
Total neutron flux at the external shield surface	$7.30 \cdot 10^{-10}$		$7.30 \cdot 10^{-10}$		$7.30 \cdot 10^{-10}$	
Untagged n flux at the external surface	$5.73 \cdot 10^{-10}$	78	$5.30 \cdot 10^{-10}$	73	$4.70 \cdot 10^{-10}$	64
Untagged n flux at the internal surface	$2.28 \cdot 10^{-11}$	4	$8.30 \cdot 10^{-12}$	2	$2.20 \cdot 10^{-12}$	0.5
Number of n in the surface of LXe in 1 year	40		15		3	

Table 1: Summary of the performances of the water shield against the muon-induced neutrons in the LNGS rock. The neutron flux is expressed in $(\text{cm}^2 \text{ s})^{-1}$ and the percentages are calculated with respect to the value of the previous line.

If now we propagate the neutrons in the water tank with 10 m height, 10 m diameter (corresponding approximately to a 4.5 m buffer all around the cryostat) and we look at the recoil spectrum in the LXe we obtain the results shown in Fig. 8: selecting single scatter, nuclear recoils there are 0.07 events per year in the 1.2 ton FDV in the 7–45 keVr energy window. Such a background can be compared directly with the nuclear recoils given by a 100 GeV WIMP, assuming a cross

section 10^{-47} cm^2 (green line): in the 7–45 keVr energy window the background is well below the expected WIMP signal.

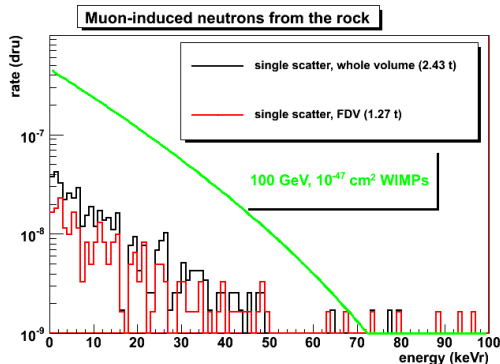


Figure 8: Energy spectrum of the single scatters nuclear recoils in the whole 2.4 ton LXe volume (black) and in the 1.2 ton fiducial volume (red) produced by the muon-induced neutrons in the rock, with the 10 m height, 10 m diameter water tank as shield and muon veto. The green line shows the expected recoil spectrum given by a 100 GeV WIMP with cross section 10^{-47} cm^2 .

Moreover the water tank will be equipped with PMTs in order to tag the muons detecting the Cerenkov light produced in water. We plan to have about 80 PMTs (8 “ diameter) in the lateral and bottom surface, to get a muon detection efficiency better than $\sim 98\%$.

Thus this source of background is reduced to a negligible level.

5. Conclusions

For the next step of the XENON program, we propose to build a detector with a total mass of 2.4 tons of LXe (1.2 fiducial): XENON1T, with an expected sensitivity of about $5 \times 10^{-47} \text{ cm}^2$ for spin-independent WIMP-nucleon scattering. To shield the detector we plan to build a 10 m height, 10 m diameter water tank, equipped with PMTs to detect muons through the Cerenkov light they emit in water. The results of the Monte Carlo simulation show that the gammas and neutrons from rock and concrete radioactivity are reduced at a completely negligible level, and the muon-induced neutrons contribute to mimic the WIMP’s signal with 0.07 events per year, which allows to reach the foreseen sensitivity of XENON1T.

References

- [1] E. Aprile *et al.*, *First Dark Matter Results from the XENON100 Experiment*, Phys. Rev. Lett. **105**, 131302 (2010).
- [2] M. Schumann (for the XENON100 coll.), *First Results of XENON100*, these proceedings.
- [3] K. Arisaka *et al.*, *XAX: a multi-ton, multi target detection system for dark matter, double beta decay and pp solar neutrinos*, Astrop. Phys. **31** (2009) 63-74, (arXiv:0808.3968).

We conclude that with this water shield the XENON1T detector is sufficiently protected against muon-induced neutrons produced in rock to reach the nominal sensitivity.

Muon-induced neutrons in the shield and cryostat Another potential source of background is given by those neutrons produced by cosmic muons when traveling through the materials of the shield, of the cryostat and of the detector itself.

Although their production is abundant, especially in the heavy materials that constitute the cryostat (stainless steel or titanium), they are mainly created inside an e.m. or hadronic shower, thus they enter into the LXe together with a large number of gammas or other particles and the probability to produce a single scatter in the fiducial volume is extremely low.

- [4] C. Levy (for the XENONIT coll.), *Shield design for the XENONIT experiment at LSM*, these proceedings.
- [5] S. Agostinelli *et al.*, GEANT4 collaboration, Nucl. Instr. Meth. Phys. Res. **A 506** (2003) 250.
- [6] H. M. Araujo *et al.*, NIM **A545**, 398 (2005).
- [7] C. Bucci *et al.*, EPJ **A 41**, 155 (2009).
- [8] H. Wulandari *et al.*, Astrop. Physics **22**, 313 (2004).
- [9] R. Lemrani *et al.*, NIM **A 560**, (2006) 454-459.
- [10] D. Mei and A. Hime, Phys. Rev. D **73**, 053004 (2006) [arXiv:astro-ph/0512125].

POS (IDM2010) 053